imatest®

Test Lab Services Report

Canon EOS 40D DSLR Sensor Characterization Based on EMVA 1288

Report ID: SAMPLE02

Requested by:

Customer

Prepared by:

Imatest, LLC

2525 Frontier Ave, Suite B, Boulder, CO 80301, USA 1-800-599-3154

Contents

2525 Frontier Ave, Suite B, Boulder, CO 80301, USA 1-800-599-3154

Overview

The EMVA 1288 standard is an initiative of the European Machine Vision Association to define a unified method for the objective measurement and analysis of specification parameters for image sensors, particularly those used in the computer vision industry. Its goal is to define reliable and reproducible measurement procedures and data presentation guidelines to simplify the comparison of cameras and image sensors. Models for both linear and non-linear sensor responses are presented in Version 4.0 of the standard.

In this report, measurements and analyses are made to quantify the linearity, sensitivity, noise, nonuniformity, and dark current of a Canon EOS 40D DSLR sensor according to the methods described in the EMVA 1288 4.0 standard.

The linear 4.0 release of the EMVA 1288 standard is only applicable to sensors that adhere to the assumptions of the linear model, which assumes that:

1. The sensor has a response that increases linearly with the number of incident photons.
2. The temporal noise is comprised only of dark noise and photon shot noise.
3. Temporal noise between pixels is statistically independent.

In comparison, the general model applies to sensors with non-linear responses or internal reprocessing, and treats the sensor or camera as a black box, assuming that:

1. The characteristic curve (sensor response) is not necessarily linear.
2. The temporal noise includes shot noise plus all unknown noise sources.
3. Temporal noise between pixels is NOT necessarily statistically independent.

These and additional assumptions are described in detail in the official standard documentation. Data capture processes for both models are identical, such that only the subsequent analyses differ them. Both the linear and general models can be applied to the Canon EOS 40D DSLR sensor, which exhibits a linear response. This report details the results obtained by each method.

For more information on the EMVA 1288 standard, visit www.emva.org.

Summary Sheet for Sensor Channel 1 at 445 nm

Type of data	14-bit RGGB	Gain	ISO 200
Exposure control	By exposure time	Environmental temp	22°C
Exposure time	1/8000 to 1 [s]	Camera body temp	---
Frame rate	---	Internal temperature(s)	---
Data transfer mode	USB 2.0	Wavelength cntr, FWHM	445 nm, 16 nm

Photon Transfer

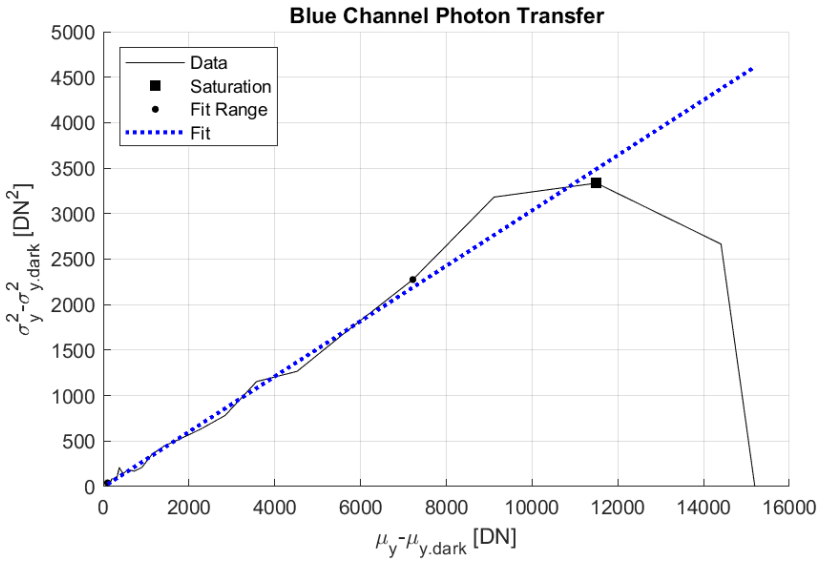

Signal-to-Noise Ratio

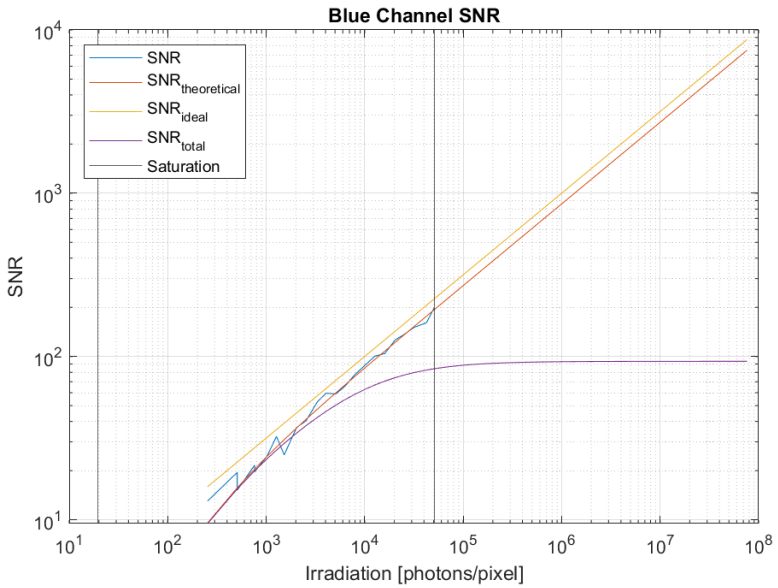

Quantum efficiency	
η	73.9%
Overall System Gain	
K	0.304 DN/e^-
1/K	3.29 e^-/DN
Temporal dark noise	
σ_d	14.0 e^-
$\sigma_{y.dark}$	4.28 DN
Signal-to-noise ratio	
SNR_{max}	194
	45.8 dB
1/ SNR_{max}	0.52%
Absolute sensitivity threshold	
$\mu_{e.min}$	14.6 e^-
$\mu_{e.min.area}$	0.45 $e^-/\mu m^2$
Saturation capacity	
$\mu_{e.sat}$	37589 e^-
$\mu_{e.sat.area}$	1153 $e^-/\mu m^2$
Dynamic range	
DR	2589
	68.3 dB
Spatial nonuniformities	
$DSNU_{1288}$	1.71 e^-
$DSNU_{1288.col}$	0.51 e^-
$DSNU_{1288.row}$	0.52 e^-
$DSNU_{1288.pix}$	1.55 e^-
$PRNU_{1288}$	1.07%
$PRNU_{1288.col}$	0.79%
$PRNU_{1288.row}$	0.50%
$PRNU_{1288.pix}$	0.52%
Linearity error	
LE	2.14%
Dark current	
$\mu_{c.mean}$	0.19 e^-/s
$\mu_{c.var}$	0.31 e^-/s

Summary Sheet for Sensor Channel 2 at 520 nm

Type of data	14-bit RGGB	Gain	ISO 200
Exposure control	By exposure time	Environmental temp	22°C
Exposure time	1/8000 to 1 [s]	Camera body temp	---
Frame rate	---	Internal temperature(s)	---
Data transfer mode	USB 2.0	Wavelength cntr, FWHM	520 nm, 35 nm

Photon Transfer

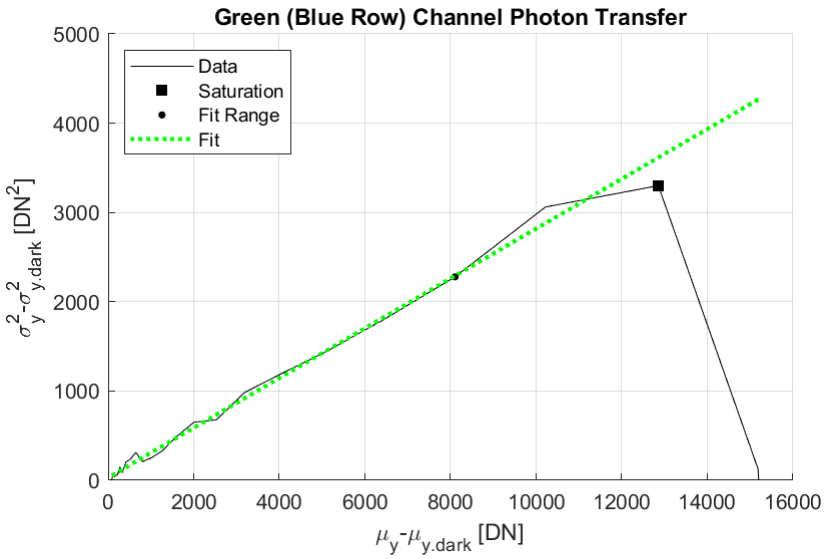

Signal-to-Noise Ratio

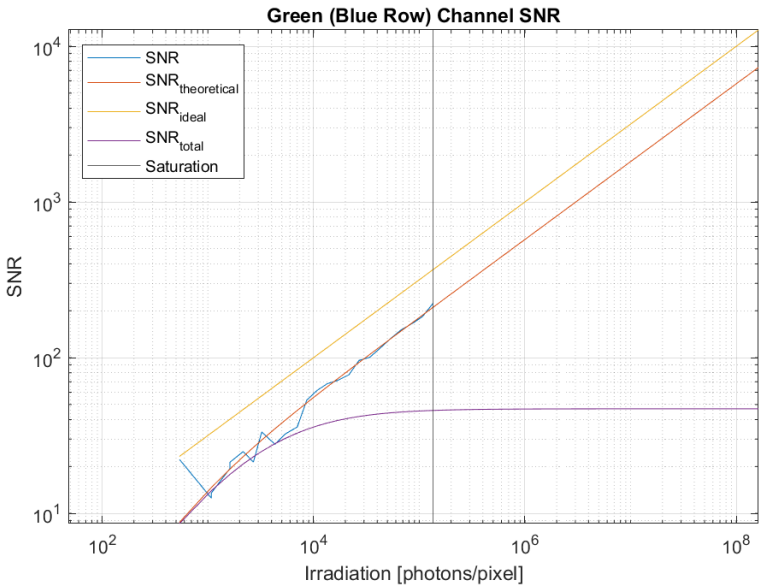

Quantum efficiency	
η	33.0%
Overall System Gain	
K	0.279 DN/e^-
1/K	3.59 e^-/DN
Temporal dark noise	
σ_d	15.3 e^-
$\sigma_{y.dark}$	4.27 DN
Signal-to-noise ratio	
SNR_{max}	211
	46.5 dB
1/ SNR_{max}	0.47%
Absolute sensitivity threshold	
$\mu_{e.min}$	15.8 e^-
$\mu_{e.min.area}$	0.49 $e^-/\mu m^2$
Saturation capacity	
$\mu_{e.sat}$	44498 e^-
$\mu_{e.sat.area}$	1365 $e^-/\mu m^2$
Dynamic range	
DR	2821
	69.0 dB
Spatial nonuniformities	
$DSNU_{1288}$	0.95 e^-
$DSNU_{1288.col}$	0.47 e^-
$DSNU_{1288.row}$	0.51 e^-
$DSNU_{1288.pix}$	0.65 e^-
$PRNU_{1288}$	2.13%
$PRNU_{1288.col}$	1.81%
$PRNU_{1288.row}$	0.97%
$PRNU_{1288.pix}$	0.57%
Linearity error	
LE	1.29%
Dark current	
$\mu_{c.mean}$	0.42 e^-/s
$\mu_{c.var}$	0.43 e^-/s

2525 Frontier Ave, Suite B, Boulder, CO 80301, USA 1-800-599-3154

Summary Sheet for Sensor Channel 3 at 520 nm

Type of data	14-bit RGGB	Gain	ISO 200
Exposure control	By exposure time	Environmental temp	22°C
Exposure time	1/8000 to 1 [s]	Camera body temp	---
Frame rate	---	Internal temperature(s)	---
Data transfer mode	USB 2.0	Wavelength cntr, FWHM	445 nm, 35 nm

Photon Transfer

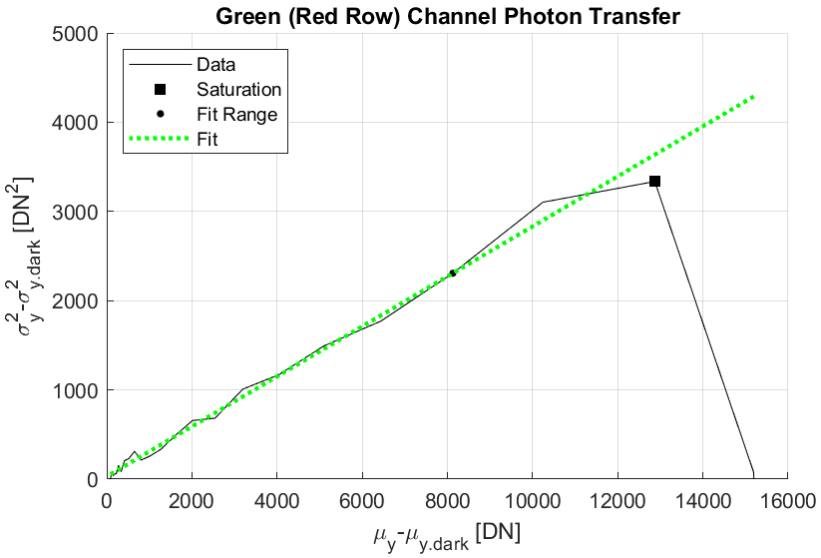

Signal-to-Noise Ratio

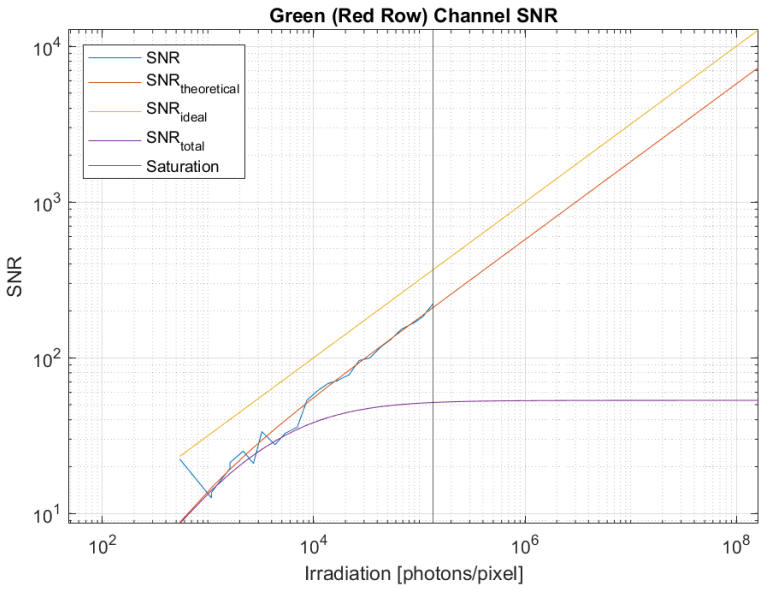

Quantum efficiency	
η	32.9%
Overall System Gain	
K	0.280 DN/e^-
1/K	3.57 e^-/DN
Temporal dark noise	
σ_d	15.3 e^-
$\sigma_{y.dark}$	4.29 DN
Signal-to-noise ratio	
SNR_{max}	211
	46.5 dB
1/ SNR_{max}	0.47%
Absolute sensitivity threshold	
$\mu_{e.min}$	15.8 e^-
$\mu_{e.min.area}$	0.49 $e^-/\mu m^2$
Saturation capacity	
$\mu_{e.sat}$	44403 e^-
$\mu_{e.sat.area}$	1362 $e^-/\mu m^2$
Dynamic range	
DR	2828
	69.0 dB
Spatial nonuniformities	
$DSNU_{1288}$	1.02 e^-
$DSNU_{1288.col}$	0.47 e^-
$DSNU_{1288.row}$	0.08 e^-
$DSNU_{1288.pix}$	0.90 e^-
$PRNU_{1288}$	1.89%
$PRNU_{1288.col}$	1.63%
$PRNU_{1288.row}$	0.77%
$PRNU_{1288.pix}$	0.54%
Linearity error	
LE	1.33%
Dark current	
$\mu_{c.mean}$	0.44 e^-/s
$\mu_{c.var}$	0.42 e^-/s

2525 Frontier Ave, Suite B, Boulder, CO 80301, USA 1-800-599-3154

Summary Sheet for Sensor Channel 4 at 635 nm

Type of data	14-bit RGGB	Gain	ISO 200
Exposure control	By exposure time	Environmental temp	22°C
Exposure time	1/8000 to 1 [s]	Camera body temp	---
Frame rate	---	Internal temperature(s)	---
Data transfer mode	USB 2.0	Wavelength cntr, FWHM	635 nm, 18 nm

Photon Transfer

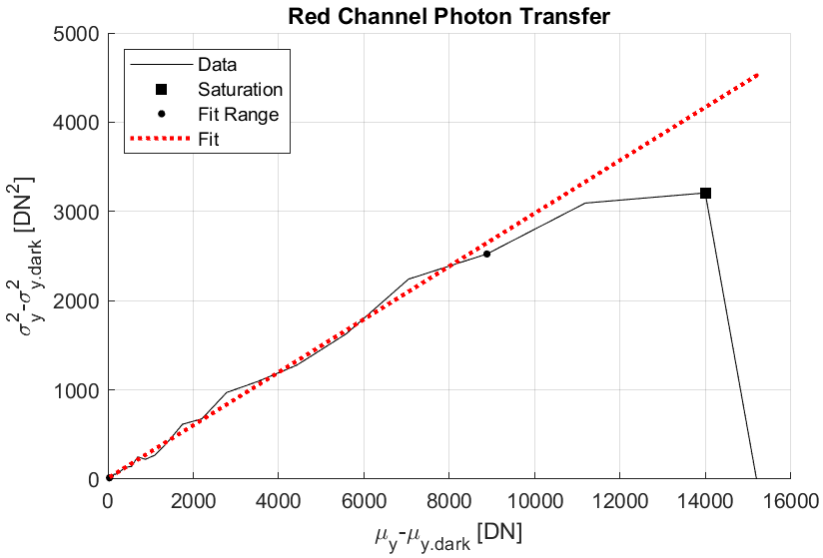

Signal-to-Noise Ratio

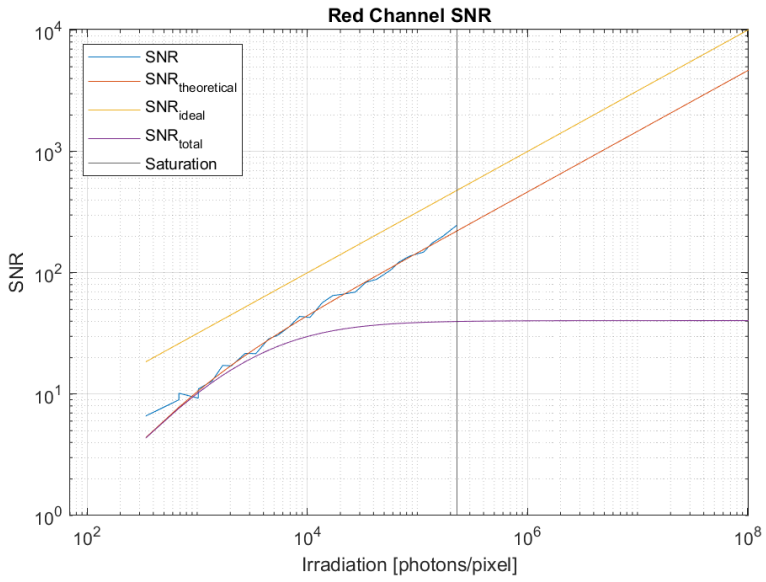

Quantum efficiency	
η	21.5%
Overall System Gain	
K	0.297 DN/e^-
1/K	3.37 e^-/DN
Temporal dark noise	
σ_d	14.4 e^-
$\sigma_{y.dark}$	4.28 DN
Signal-to-noise ratio	
SNR_{max}	221
	46.9 dB
1/ SNR_{max}	0.45%
Absolute sensitivity threshold	
$\mu_{e.min}$	14.9 e^-
$\mu_{e.min.area}$	0.46 $e^-/\mu m^2$
Saturation capacity	
$\mu_{e.sat}$	49018 e^-
$\mu_{e.sat.area}$	1503 $e^-/\mu m^2$
Dynamic range	
DR	3302
	70.4 dB
Spatial nonuniformities	
$DSNU_{1288}$	0.83 e^-
$DSNU_{1288.col}$	0.56 e^-
$DSNU_{1288.row}$	0.08 e^-
$DSNU_{1288.pix}$	0.60 e^-
$PRNU_{1288}$	2.47%
$PRNU_{1288.col}$	2.22%
$PRNU_{1288.row}$	0.83%
$PRNU_{1288.pix}$	0.71%
Linearity error	
LE	1.99%
Dark current	
$\mu_{c.mean}$	0.37 e^-/s
$\mu_{c.var}$	0.42 e^-/s

2525 Frontier Ave, Suite B, Boulder, CO 80301, USA 1-800-599-3154

Device Details

Table 1: Device Summary

Spec	Canon EOS 40D
Sensor Type	CMOS
Sensor Size	22.2 x 14.8 mm
Pixel Dimensions	3888 x 2592
MP	10.1
F/#	f/9.2
Pixel Pitch	5.71 µm

2525 Frontier Ave, Suite B, Boulder, CO 80301, USA 1-800-599-3154

Test Capture Setup

Linearity, Sensitivity, and Noise

Test Distance: 1.4 m
Target: Thouslite LED Cube; Blue (445 [nm]), Green (520 [nm], and Red (635 [nm]) light channels
Device Settings: No lens, ISO 200, Shutter Speed 1/640 [s]

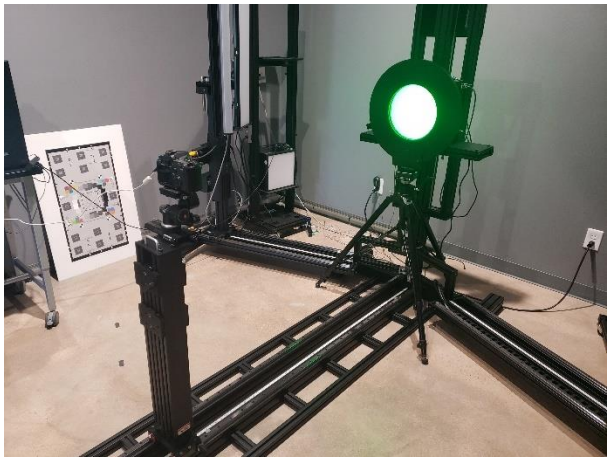

Figure 1: Hardware setup

The Thouslite LED Cube is a tunable light source with 15 individually controllable LED channels covering a spectral range of 350-700 [nm]. The hardware setup for linearity, sensitivity, and noise measurements is shown in Figure 1. The lensless device is mounted on the Imatest Modular Test Stand, 1400 [mm] from sensor to illumination surface. An adjustable aperture flush with the light source is set to a 175 [mm] diameter.

The spectral properties of the irradiation correspond with the maximum response from each sensor channel (RGGB). The spectral distribution of each lighting condition (blue, green, and red light) is measured using a Jeti Specbos spectrometer positioned on the same plane as the image sensor, calibrated in units of irradiance [W/m^2]. The peak wavelengths of each condition and corresponding spectra are shown in Table 2 and Figure 2, respectively. Two images are captured at each of 40 different exposures using constant illumination and shutter speeds ranging from 1/8000 to 1 [s]. Note that this results in exposures that are not equally spaced, but this has little effect on the resulting analysis due to the logarithmic nature of exposure.

Table 2: Peak Illumination Wavelengths

Sensor Channel	Peak λ [nm]
Blue	445
Green (B)	520
Green (R)	520
Red	635

2525 Frontier Ave, Suite B, Boulder, CO 80301, USA 1-800-599-3154

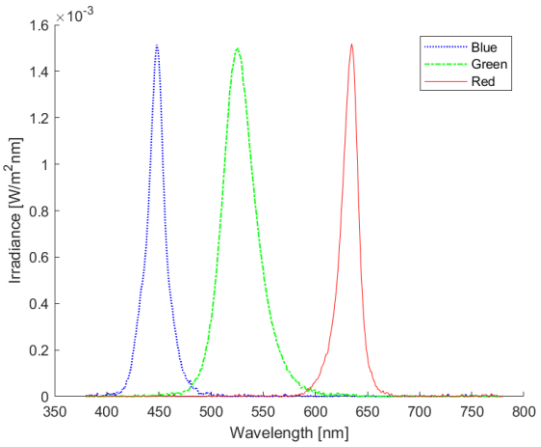

Figure 2: Spectra of the blue, green, and red LED channels used to illuminate the camera sensor

Dark Current

Test Distance: N/A
Target: Dark, lens cap on
Device Settings: No lens, lens cap on, ISO 200, all shutter speeds ranging from 1/8000 up to 30 [s].

Measurements for dark current at a single temperature were conducted in a lab setting at room temperature of 22 degrees Celsius. Dark images were captured for all available shutter speeds on the device, ranging from 1/8000 up to 30 [s]. An ISO of 200 was used, and two images are captured for each exposure time.

Nonuniformity

Lighting Conditions: Thouslite LED Cube system, 6103K, 1002 lux
Test Distance: 0.31m (not critical to measurement)
Chart: Calibrite ColorChecker Classic

Data capture for spatial nonuniformity is conducted under the same conditions as the linearity, sensitivity, and noise measurements. Quantities related to most nonuniformities are evaluated using the mean gray values averaged over a large number of images in order to suppress temporal noise. Analysis is completed using an averaged set of dark images and an averaged set of images at 50% saturation. A constant shutter speed of 1/60 [s] is used to capture both dark and half-saturation images for the blue, green, and red channels. To achieve 50% saturation under the various illuminations, intensity values were adjusted for each illumination to achieve a mean digital number that was 50% of the maximum saturation. For a 14-bit sensor, saturation occurs at 16225 [DN], so half saturation images with a mean of 8112 [DN] were captured. One hundred dark images were captured in addition to one hundred half-saturation images under each illumination.

Analysis Results and Observations

Linearity, Sensitivity, and Noise

Photon Transfer Curve

The photon transfer curve, shown for each channel in Figure 3, represents the relationship between mean photon-induced gray values and the corresponding variance. The slope of this curve is the gain, K, or amplification of the system, described by:

$$\sigma_y^2 = \sigma_{y.dark}^2 + K\left(\mu_y - \mu_{y.dark}\right) \quad (1)$$

where μ_y is the average gray value over all pixels in an image captured at a particular time. The mean is computed from the two images captured at the same exposure time. This process is also applied to the dark images, yielding $\mu_{y.dark}$. From these same images, the temporal variance σ_y^2 is calculated and similarly for the darks to determine $\sigma_{y.dark}^2$.

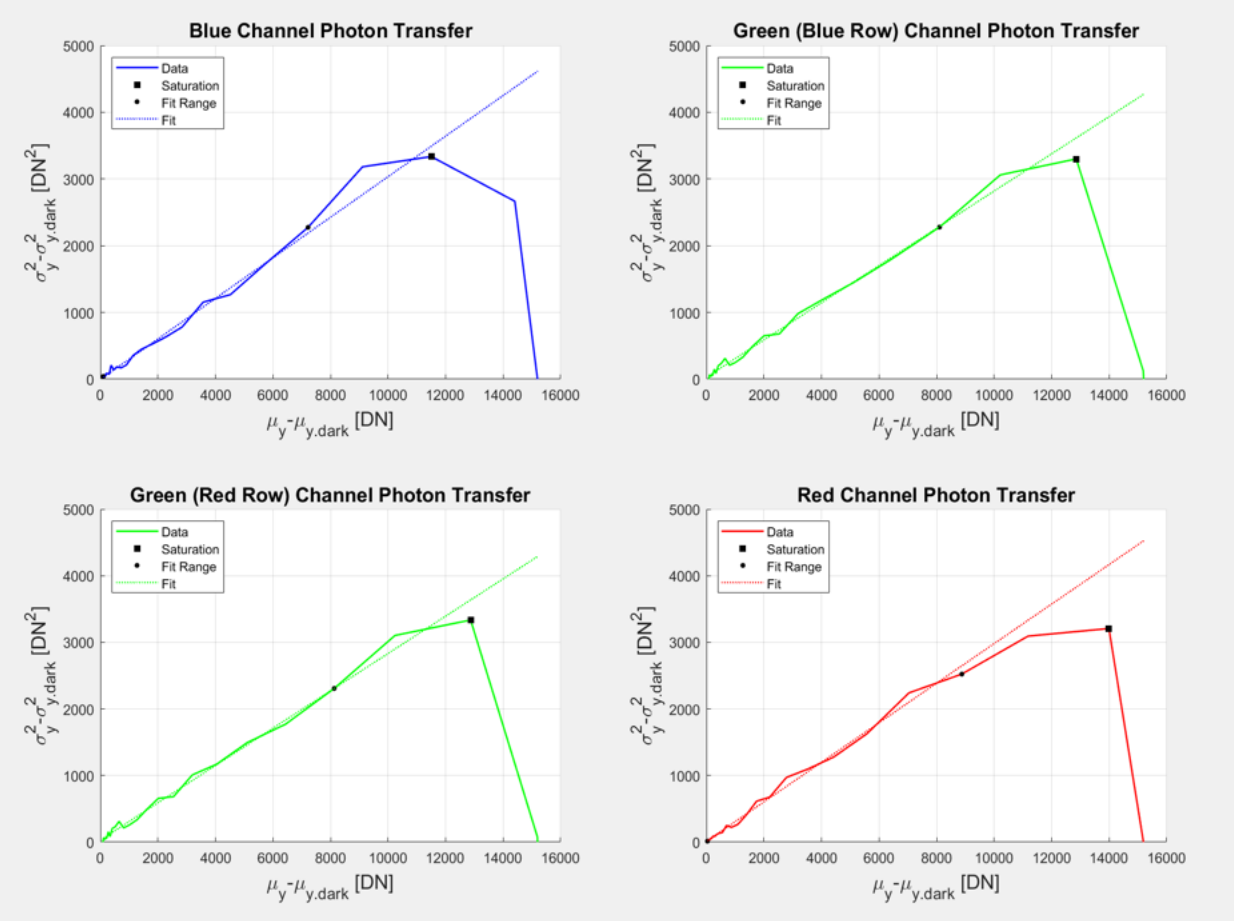

Figure 3: Photon transfer curves for each of the four sensor channels

Gain is a quantity used to describe camera electronics related to the conversion of photons to a voltage, which is amplified and converted into a digital signal. For a linear process as shown, there is a single gain value, or slope, that describes the system. Each channel is analyzed separately due to wavelength dependencies, including each of the two green channels to identify potential discrepancies. It is not expected for any digital sensor to be perfectly linear due to inevitable sources of error and noise. The linear trend deviates upon nearing, and eventually fails at, the point of saturation, as shown in Figure 3. To obtain a single slope value for the gain, a linear regression is fitted to the data ranging from the minimum value up to 70% of the value of saturation. For nonlinear systems, due to the black box nature of the system, the photon transfer curve—and therefore the gain—cannot be calculated.

The gain values for each channel are summarized in Table 3.

Table 3: Photon Transfer Curve Gain

Sensor Channel	Gain, K [DN/e^2]
Blue	0.304
Green (B)	0.279
Green (R)	0.280
Red	0.297

Characteristic Curve

The sensitivity, or characteristic curve, shown for each channel in Figure 4, is the relationship between the mean gray value and mean number of photons per pixel. The slope of this curve yields the responsivity, R.

Linear Model

In the linear model, the characteristic curve is described as

$$\mu_y - \mu_{y.dark} = R\mu_p \tag{2}$$

where μ_y and $\mu_{y.dark}$ are the average gray values, and μ_p is the quantum exposure, in photons, which is calculated from the radiance at the sensor plane. Resulting curves, shown in Figure 4, are fitted using a linear least squares regression. The responsivity values for each channel are summarized in Table 4.

Table 4: Characteristic Curve Responsivity

Sensor Channel	Responsivity, R [DN/p]
Blue	0.225
Green (B)	0.092
Green (R)	0.092
Red	0.064

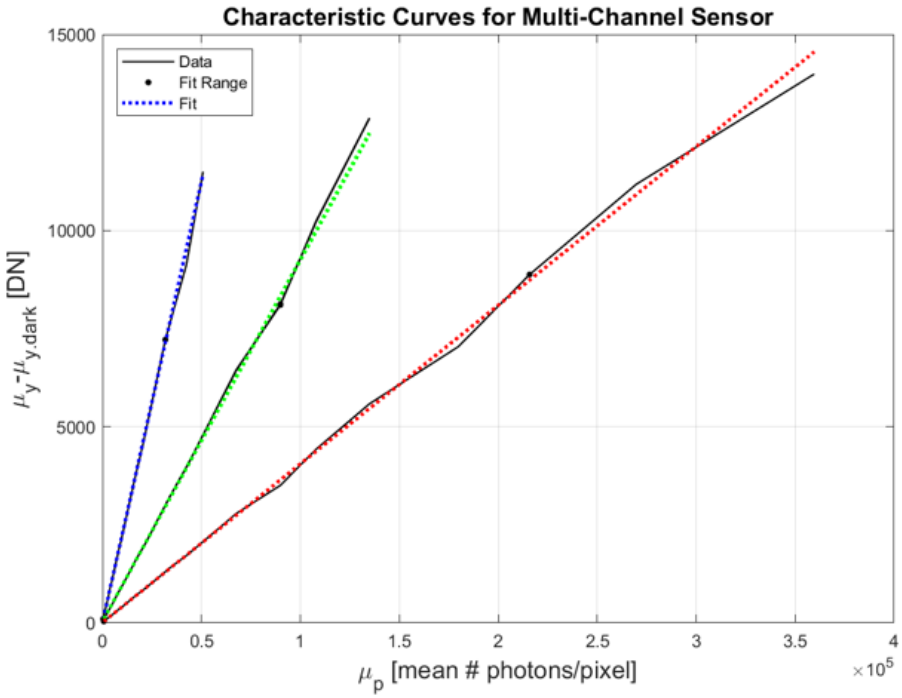

Figure 4: Characteristic curves, also called sensitivity curves, for each of the four sensor channels

The ratio of these two resultant quantities from the linear photon transfer and characteristic curves—responsivity, R, over gain, K—yields the quantum efficiency, η, the percentage of photons incident on a photodiode that generates an electric charge, summarized in Table 5. QE and gain are also used in the final calculation of SNR.

Table 5: Quantum Efficiency

Sensor Channel	QE
Blue	0.739
Green (B)	0.330
Green (R)	0.329
Red	0.215

General Model

Because the general model can be used for nonlinear response sensors, the characteristic curve is fitted using a cubic B-spline regression in the form:

$$\mu_y - \mu_{y.dark} = \sum_{p=0}^{P+2} \alpha_p \beta_3 \left(\frac{\mu_p}{\Delta\mu_p} - (p-1) \right) \quad (3)$$

here α_p are the regression parameters for the cubic B-splines, β_3, fit to the curve over P intervals of width $\Delta\mu_p = \mu_{p.sat}/P$. The photon-dependent responsivity is the instantaneous slope, or derivative, of the curve.

Linearity

Linearity is determined by computing a least-squares linear regression of the characteristic curve in the range between 5% and 95% of the saturation capacity, shown in Figure 5. The relative deviation from the fit, plotted in Figure 6, is then calculated as:

$$\delta_y[i]\ [\%] = 100\frac{y[i] - (a_0 + a_1 H[i])}{(a_0 + a_1 H[i])} \quad (4)$$

where $(a_0 + a_1 H[i])$ is the linear relation with offset a_0, slope a_1, and exposure values $H[i]$. $y[i]$ is the dark subtracted mean number of photons for a particular data point. The linearity error is calculated as the mean of the absolute deviation in the 5% to 95% range of saturation capacity, summarized for each channel in Table 6.

Table 6: Linearity Error

Sensor Channel	Linearity Error, LE [%]
Blue	1.86
Green (B)	0.936
Green (R)	0.974
Red	1.97

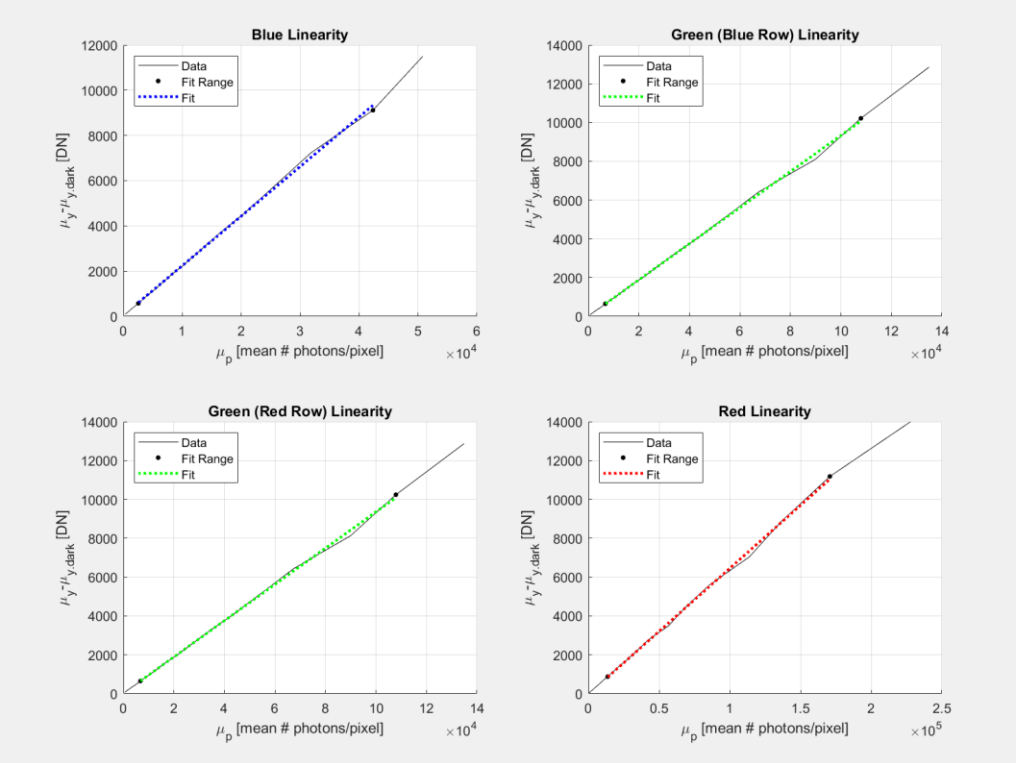

Figure 5: Linear least squares regression fit from 5% to 95% of the saturation capacity range

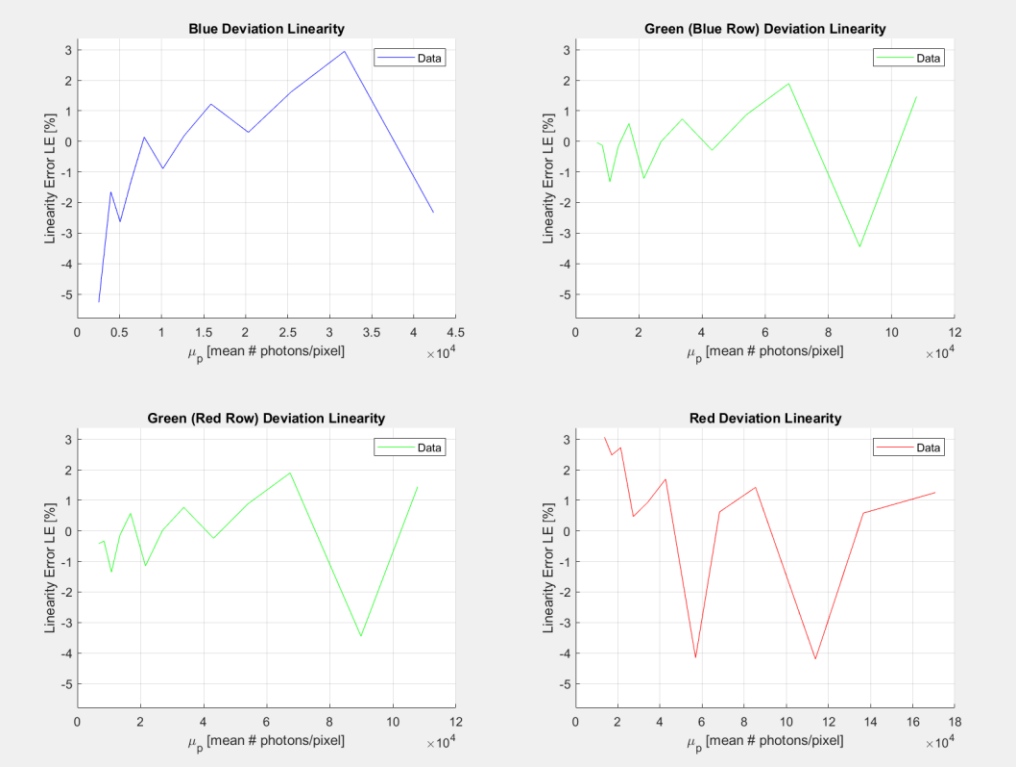

Figure 6: Relative deviation from linear fit

Dark Current

Dark current can be computed from either the mean or the variance. The mean is preferred because it can be more accurately estimated, but the variance calculation is useful for systems that feature dark current compensation. The resulting mean dark signal [DN] and the variance in dark signal [DN^2] are plotted against exposure time in Figure 7. The slope of the mean dark signal relation is the dark current, which is determined by performing a linear least squares regression on the data points. The dark current results for each channel are summarized in Table 7. Note that the square root of the variance calculation is taken to compare both results in the same units.

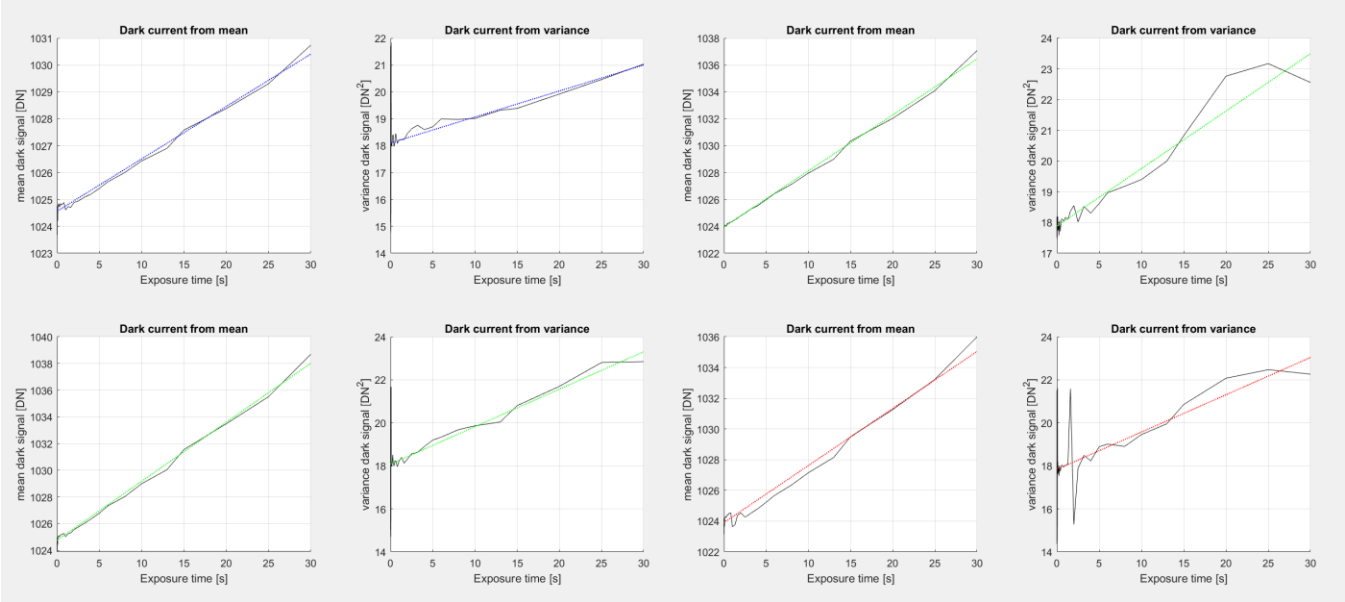

Figure 7: Dark current for each channel calculated from mean and variance

Table 7: Average Dark Current

Dark Current	Blue	Green (B)	Green (R)	Red
From Mean [DN/s]	0.195	0.416	0.442	0.371
From Variance [DN/s]	0.311	0.432	0.417	0.416

Nonuniformity

The last set of required measured measurements for the standard involves the characterization of sensor nonuniformities. Figure 8 shows a scaled image captured by Camera 1 at 50% saturation. The dark circular spots reveal dust on the sensor, and there is obvious vignetting around the edges and corners. Of particular interest are the vertical lines visible in the image. In CMOS sensors, these lines are typically the result of fixed pattern noise due to the individual amplifiers on each column. Slight differences in amplification across columns of pixels result in these variations in the output signal.

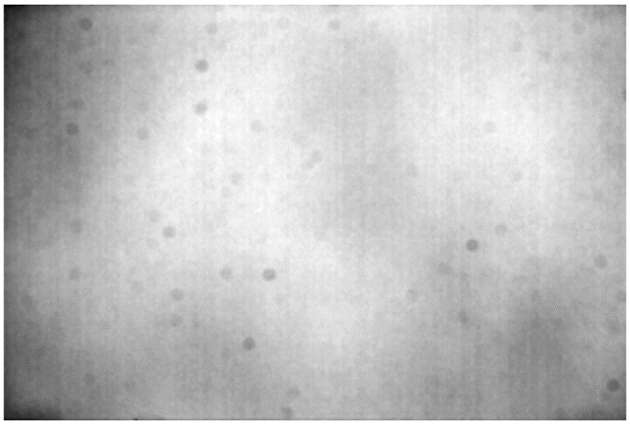

Figure 8: Scaled image captured at half-saturation

Objective characterization of nonuniformity utilizes a descriptor called photo-response nonuniformity (PRNU), summarized for each channel in Table 8, which describes the variation in gain across a sensor by analyzing the frequency information of the captured images. Spectrograms, shown in Figure 9, are calculated by taking the one-dimensional Fourier transform of an image in either the horizontal or vertical direction, and then computing the mean power spectrum of that result. As before, these calculations are done for each channel. In Figure 9, short peaks visible in the vertical spectrograms correspond with the frequencies of the column noise.

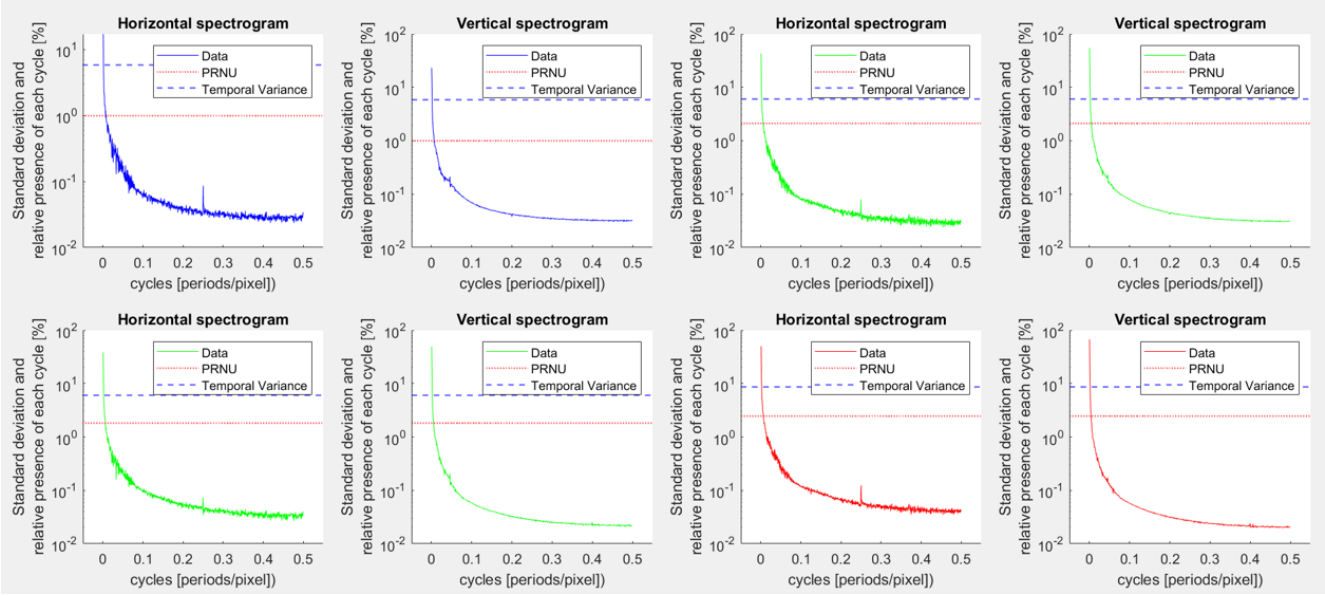

Table 8: PRNU

PRNU [%]	Blue	Green (B)	Green (R)	Red
$PRNU_{1288}$	1.07	2.13	1.88	2.47
$PRNU_{1288.col}$	0.786	1.81	1.63	2.22
$PRNU_{1288.row}$	0.503	0.965	0.773	0.827
$PRNU_{1288.pix}$	0.524	0.571	0.536	0.712

A similar computational process is applied to the series of dark captures to yield dark-signal nonuniformity (DSNU). DSNU characterizes the fluctuation in bias, which is the effect in many image sensors where, even without light, pixels may have a non-zero value. Due to inevitable variations of noise in imaging detectors, many sensors add an offset to prevent the digital signal from dropping below zero, but it is not always equal across all pixels in a sensor, or over time. Figure 10 shows a dark image captured with the device, again scaled to make the noise more apparent. Close examination reveals hot pixels, which appear fully saturated, and a horizontal banding pattern. Corresponding spectrograms are shown in Figure 11. Temporal, or random noise, dominates, but there are spikes that indicate fluctuation in bias across the sensor.

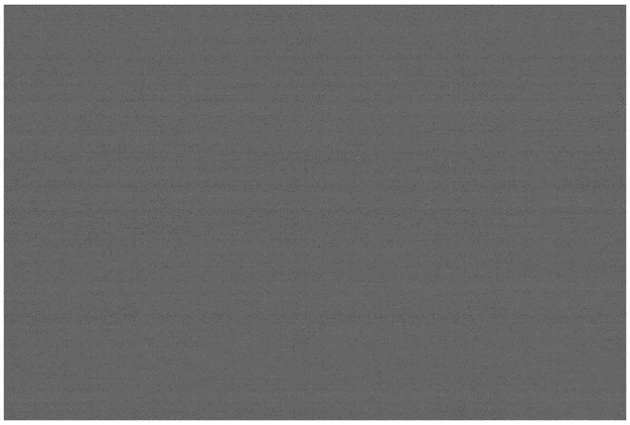

Figure 10: Scaled dark image scaled to reveal extent of sensor nonuniformities. Close examination reveals hot pixels and a horizontal banding pattern

Table 9: DSNU

DSNU [e^-]	Blue	Green (B)	Green (R)	Red
$DSNU_{1288}$	5.63	3.39	3.62	2.79
$DSNU_{1288.col}$	1.67	1.68	1.67	1.89
$DSNU_{1288.row}$	1.71	1.83	0.297	0.286
$DSNU_{1288.pix}$	5.10	2.31	3.21	2.03

2525 Frontier Ave, Suite B, Boulder, CO 80301, USA 1-800-599-3154

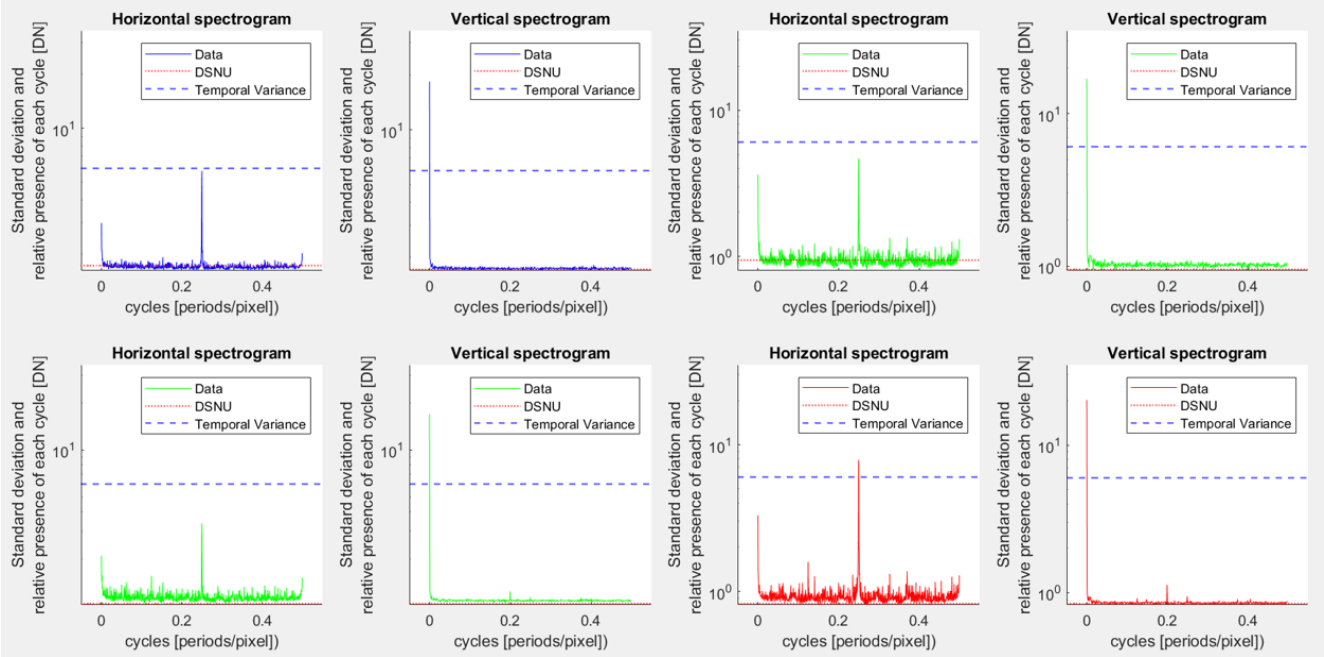

Figure 11: Vertical and horizontal spectrograms calculated from dark images for each channel

SNR Analysis

These measurements and quantities come together in the calculation of the total SNR. The linear SNR model incorporates quantum efficiency, η, the incident number of photons, μ_p, temporal dark noise, σ_d^2 , the DSNU and PRNU, gain, K, and readout noise, σ_q^2.

$$SNR_{tot}(\mu_p) = \frac{\eta\mu_p}{\sqrt{\sigma_d^2 + DSNU^2 + \frac{\sigma_q^2}{K^2} + \eta\mu_p + PRNU^2(\eta\mu_p)^2}} \quad (5)$$

Without known efficiency or gain values, the total SNR for the general model is calculated as:

$$SNR_{p.tot}(\mu_p) = \frac{\mu_p}{\sqrt{\sigma_p^2(\mu_p) + s_p^2(\mu_p)}} \quad (6)$$

Linear SNR curves are plotted in Figure 12. Notice that when considering the DSNU and PRNU in the total SNR, there is a falloff in SNR as the irradiation increases and approaches saturation, as opposed to the theoretical SNR. Equations for the various forms of SNR are defined in the standard documentation. Increased variation in the SNR at lower irradiation is due to the larger number of data points taken at shorter exposure times.

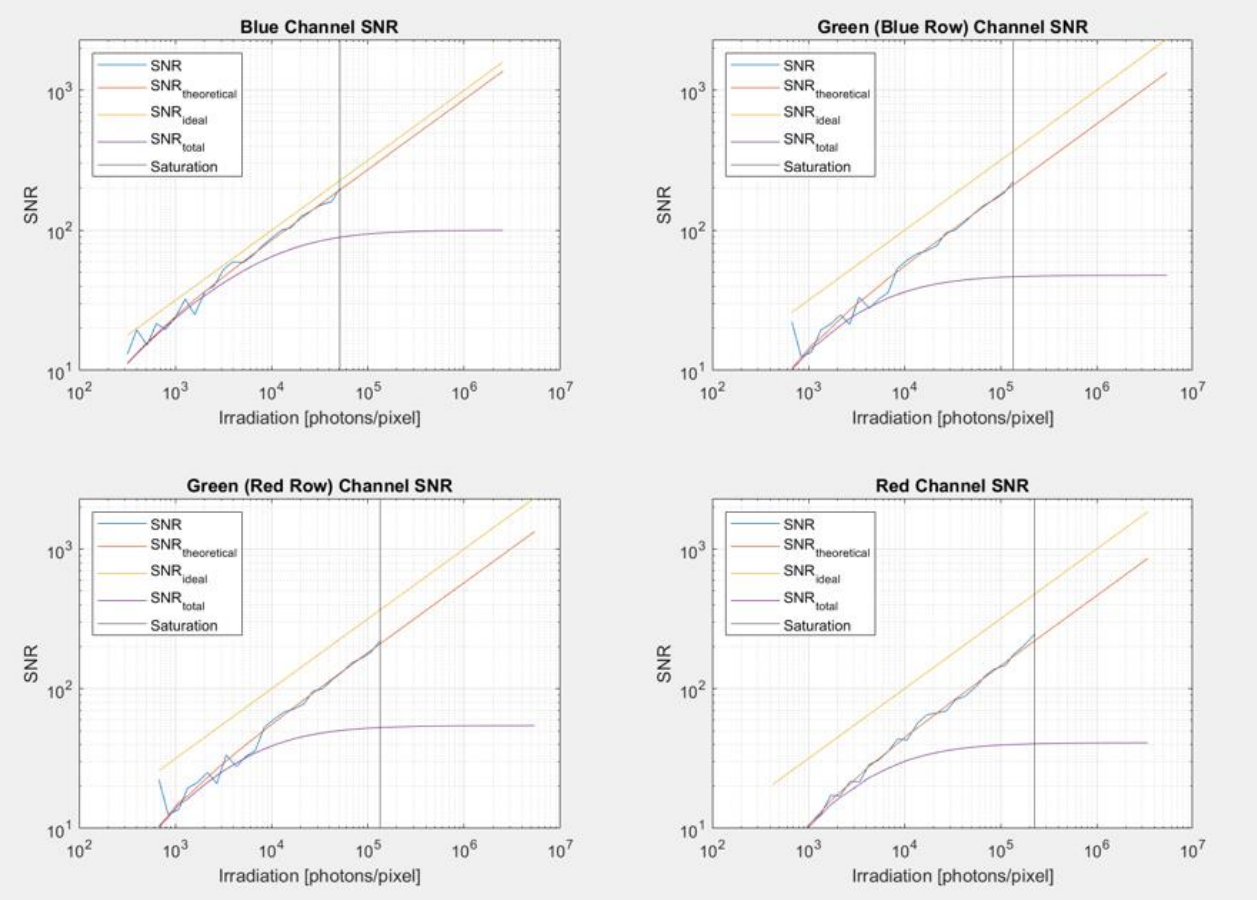

Figure 12: Signal-to-Noise Ratio (SNR) channel based on combination of calculated parameters.